

Performance Testing of Massive MIMO Base Station with Multi-Probe Anechoic Chamber Setups

Fengchun Zhang¹, Wei Fan¹, Yilin Ji¹, Mattias Gustafsson²,
Tommi Jamsa², Gerhard Steinböck², Pekka Kyösti³, and Gert F. Pedersen¹

¹APMS section, Department of Electronic Systems, Aalborg University, Denmark,

E-mail: {fz, wfa, yilin, gfp}@es.aau.dk

²Huawei Technologies Sweden AB, Gothenburg, Sweden,

E-mail: {Mattias.Gustafsson, tommi.jamsa, gerhard.steinbock}@huawei.com

³Keysight Technologies and Oulu University, Finland, E-mail: pekka.kyosti@keysight.com

Abstract—The utilization of massive multiple-input multiple-output (MIMO) antenna arrays at the base station (BS) side has been identified as an enabling technique for 5G communication systems. To evaluate the true end-to-end performance of BS's, an over-the-air (OTA) radiated method is required. In this paper, we present a sectorized multi-probe anechoic chamber (MPAC) configuration equipped with a switch box for massive MIMO BS OTA testing. Simulations were performed for a BS equipped with an 8×8 planar array of half-wavelength element spacing at 3.5 GHz, where 1 m measurement range and 8 active OTA probes are considered. Due to the important role of beamforming techniques in 5G antenna arrays, the Bartlett beamforming power patterns under the channel models reproduced in the MPAC setups are utilized to quantify the channel emulation accuracy.

Index Terms—antenna arrays, MIMO systems, performance testing, multi-probe anechoic chamber (MPAC).

I. INTRODUCTION

Massive multi-input multi-output (MIMO) systems have been identified as an enabling technique for 5G, where a base station (BS) is equipped with a very large number of antennas. Massive MIMO BS's serve many spatially distributed terminals simultaneously in the same time-frequency resource [1].

Due to practical reasons, e.g. unavailability of temporary antenna connectors on the integrated units and a large number of antennas, it is predicted that conducted testing is no longer applicable for 5G BS's. The testing will eventually move to over-the-air (OTA) methods. Currently proposed OTA methods, i.e. radiated two-stage (RTS) or wireless cable methods, have the similar functionality as conductive testing, by calibrating out the transfer matrix between the channel emulator (CE) antenna ports and the device under test (DUT) antenna ports [2], [3]. However, these two methods are not true end-to-end testing methods, because the actual antenna radiated patterns are calibrated out and not inherently included during testing. Further, they are not capable of testing adaptive antenna systems. The system complexity and cost would be extremely high due to the large number of required OTA antennas, which is proportional to DUT antenna number.

One cost-effective method for true end-to-end testing is the reverberation chamber (RC) method [4]. This method can be

considered as isotropic environments. However, RC could not offer any practical or realistic test environment that reflects an expected usage scenario.

The promising candidate for massive MIMO BS performance testing is the multi-probe anechoic chamber (MPAC) method [5]–[7]. The MPAC method is technically sound for massive MIMO BS testing. Arbitrary radio frequency (RF) environments can be emulated in the test area to properly evaluate the performance of MIMO BS's. However, when examining the feasibility of MPAC for 5G BS testing, one big concern is the overwhelming cost of 3D MPAC setup. The design of the MPAC system directly determines the cost, including range between OTA probes and DUT center, the OTA probe configuration, and the number of active OTA probes, etc. Thus an MPAC setup that can meet the requirement for 5G BS testing with an acceptable system cost is needed.

In this paper, a 3D sectorized MPAC setup with a limited number of active probes and using pre-faded signal synthesis (PFS) technique is proposed for massive MIMO BS OTA testing. The proposed MPAC system can not only cover the angular space in which BS's mainly focus on, but also has the potential to reduce the total system cost, via reducing the required number of fading CEs, respective hardware resource and the size of the chamber. The key design parameters to be determined include the measurement range (distance between the OTA probes and DUT center), the OTA probe configuration (the number and locations of OTA probes), and the number of active OTA probes. Note that the Bartlett beamforming patterns correspond to matched filter method in massive MIMO, thus this is an important criterion. Therefore we use as one figure of merit (FoM) the Bartlett beamforming power patterns reproduced in the MPAC setups to evaluate the channel emulation accuracy.

II. PROPOSED MPAC CONFIGURATION

The proposed MPAC configuration for the massive MIMO BS OTA testing is shown in Fig. 1. The system consists of:

- an anechoic chamber, which is used to shield external unwanted interference and unintended reflections inside

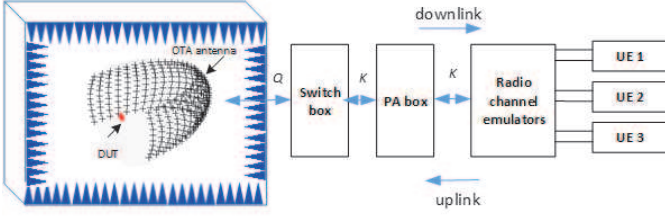


Fig. 1. The proposed MPAC setups for radiated performance testing of massive MIMO BS.

the anechoic chamber. The chamber dimension is largely determined by the measurement range L .

- a large set of OTA probe antennas (Q) on the sector angle of interest with equal distance L . The angular region for the sector of interest is $[-90^\circ, 90^\circ]$ and $[-30^\circ, 30^\circ]$ in azimuth and elevation, respectively.
- a uniform planar array as the massive MIMO DUT, which is placed on the vertical plane at one end of the anechoic chamber.
- a switch box, which switches the K active probe antennas from the Q probe elements to the fading emulator RF interfaces.
- a controller, which controls the switch box. It basically determines how to connect the K CE RF interface ports to the Q probes. For the standard channel models, e.g. TR 38.901, the probe selection can be done offline since the channel cluster parameters are fixed for link simulations. However, real time probe selection might be needed for dynamic channel models, e.g. with time-variant spatial profiles.
- UEs (or emulators), which are used to mimic user terminal behavior.

It is noted that practical aspects related to the setups, e.g. expected requirements on the switch, such as port isolation, input/output signal levels, bidirectional, circulators integrated in the switch box or outside, etc., are not discussed in the paper.

III. FoM

With the PFS technique, we optimize the average power weights for probes to reconstruct the target spatial channel profile within the test zone [8]. In the following discussion, both OTA and DUT antennas are assumed to be isotropic. The spatial correlation matrix of a DUT with M antennas is calculated for the ideal target model as

$$\mathbf{R} = \oint \mathbf{a}(\Omega)P(\Omega)\mathbf{a}^H(\Omega)d\Omega, \mathbf{R} \in \mathbb{C}^{M \times M}, \quad (1)$$

where $P(\Omega)$ is the continuous power angular spectrum (PAS) of the target channel model, $(\cdot)^H$ represents the Hermitian operation and $\mathbf{a}(\Omega) \in \mathbb{C}^{M \times 1}$ denotes the array factor of DUT

to the space angle Ω under the far field assumption. The m -th entry of $\mathbf{a}(\Omega)$ with $\Omega = (\theta, \phi)$ can be given as

$$\begin{aligned} a_m(\theta, \phi) &= \exp(j\Psi(\theta, \phi) \cdot \Upsilon_m^H), \\ \Psi(\theta, \phi) &= \frac{2\pi}{\lambda} [\cos \theta \cos \phi, \cos \theta \sin \phi, \sin \theta], \\ \Upsilon_m &= [x_m, y_m, z_m], \end{aligned} \quad (2)$$

where $\Psi(\theta, \phi)$ is the wave vector with θ and ϕ representing elevation and azimuth angle, respectively, λ is the wave length and Υ_m is the location vector of the m -th antenna of the DUT.

By applying the weight vector $\mathbf{W}(\Omega) = \mathbf{a}^H(\Omega)$, the Bartlett beamforming power patterns under the target channel model can then be given as

$$B(\Omega) = \mathbf{a}^H(\Omega)\mathbf{R}\mathbf{a}(\Omega). \quad (3)$$

The spatial correlation matrix under the MPAC emulated channel model is

$$\underline{\mathbf{R}} = \sum_{k=1}^K \underline{\mathbf{a}}(\Omega_k)P(\Omega_k)\underline{\mathbf{a}}^H(\Omega_k), \underline{\mathbf{R}} \in \mathbb{C}^{M \times M}, \quad (4)$$

where $P(\Omega_k)$ is the discrete power transmitted by the k -th OTA probe and $\underline{\mathbf{a}}(\Omega_k) \in \mathbb{C}^{M \times 1}$ denotes the array factor of DUT to the space angle Ω_k in the MPAC setup. The m -th entry of $\underline{\mathbf{a}}(\Omega_k)$ is written as

$$\underline{a}_m(\Omega_k) = l(d_{k,m}) \exp\left(j\frac{2\pi}{\lambda}d_{k,m}\right), \quad (5)$$

where $d_{k,m}$ is the distance between the k -th OTA probe and the m -th DUT antenna element, and $l(d_{k,m})$ is the path loss term normalized with the measurement range L , i.e.,

$$l(d_{k,m}) = \left(\frac{\lambda}{4\pi d_{k,m}}\right) / \left(\frac{\lambda}{4\pi L}\right). \quad (6)$$

By choosing the weight vector $\mathbf{W}(\Omega) = \mathbf{a}^H(\Omega)$, the Bartlett beamforming power patterns under the emulated channel model can be obtained as

$$\underline{B}(\Omega) = \mathbf{a}^H(\Omega)\underline{\mathbf{R}}\mathbf{a}(\Omega). \quad (7)$$

In this paper, our target is to select a subset of K active OTA probes within the MPAC setup and optimize the power gain of the K OTA probes to emulate the channel as close as possible to the target channel, i.e. $\underline{\mathbf{R}} \approx \mathbf{R}$ and thus $\underline{B}(\Omega) \approx B(\Omega)$. In the following, two FoMs are utilized to determine the aforementioned MPAC design parameters.

A. Power loss

Assume a single cluster is impinging on the DUT from direction Ω_T (i.e. the centroid of the cluster), the fixed beam power loss (FBPL) caused by the measurement range is

$$P_{loss} = \frac{B(\Omega_T)}{\underline{B}(\Omega_T)}. \quad (8)$$

B. Beam pattern similarity

To evaluate the similarity between the target and emulated beamforming power patterns, the similarity of the beamforming power patterns is defined as

$$S = (1 - D_p) \times 100\%, \quad (9)$$

where D_p is the pattern distortion factor defined in [9], as

$$D_p = \frac{1}{2} \int \left| \frac{B(\Omega)}{\int B(\Omega') d\Omega'} - \frac{\underline{B}(\Omega)}{\int \underline{B}(\Omega') d\Omega'} \right| d\Omega. \quad (10)$$

The range of S is $[0, 1]$, where 0 and 1 correspond to full dissimilarity and complete similarity, respectively.

IV. MPAC DESIGN FOR TR 38.901 CDL MODELS

A BS configured as an 8×8 uniform planar array with $\lambda/2$ spacing is selected as the DUT. The carrier frequency is set to 3.5 GHz. Note that other frequencies can be emulated, too.

A. Determine the measurement range L

To restrict the size of the MPAC setup, the OTA probes are close to the BS array and thus the array experiences spherical wavefronts instead of plane wavefronts, i.e., $\underline{\mathbf{a}}(\Omega_k)$ in (4) is the near field array factor of the DUT. However, the steering weight vector $\mathbf{W}(\Omega)$ is still chosen based on the far field array factor as in equation (7) to form the beam. Meaning that in the incident direction, the spherical waves weighted by $\mathbf{W}(\Omega)$ are summed partly incoherently and this results in a power loss and beam pattern distortion.

As discussed in [7], the maximum phase deviation between the spherical wave and the plane wave occurs when the impinging specular path is from the boresight direction of the DUT, where the maximum phase deviation would lead to the maximum FBPL. The most critical case in terms of FBPL is when the target channel is a specular path impinging from the DUT boresight direction. Therefore, we plot the FBPL for the aforementioned most critical scenario with various measurement ranges L in Fig. 2. We can further check the beam pattern distortion by plotting beam pattern similarity S for a boresight specular path with various L , which is shown in Fig. 3. By observing Fig. 2 and 3, we can find out that with the smaller L , the FBPL becomes higher and beam pattern similarity drops, i.e., the beam pattern distortion becomes more severe. The far field boundary, i.e., $L_b = \frac{2D^2}{\lambda}$ with D representing the aperture of DUT, is illustrated by the blue dash line in the figures. We can see that the FBPL around 0.05 dB and beam pattern similarity of 99.4% can be achieved with the measurement range set to the far field boundary. Based on Fig. 2 and 3, we can determine the measurement range L , if the acceptable FBPL or beam pattern similarity is given. For the simulations hereafter, $L = 1$ m is set, which indicates an FBPL around 0.9 dB and a pattern similarity of approximately 90%. It is noted that the pattern similarity might decrease further if a limited number of OTA probe antennas is active, as discussed later.

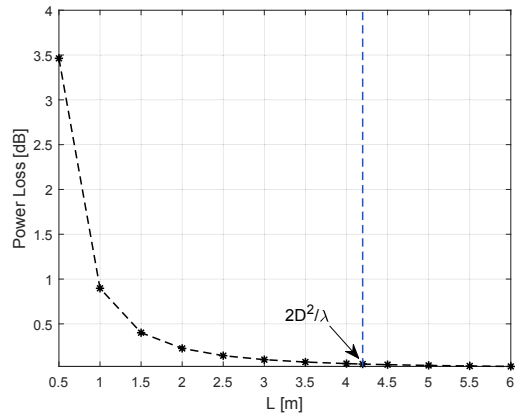


Fig. 2. The FBPL for a specular path from DUT boresight direction with various measurement ranges L .

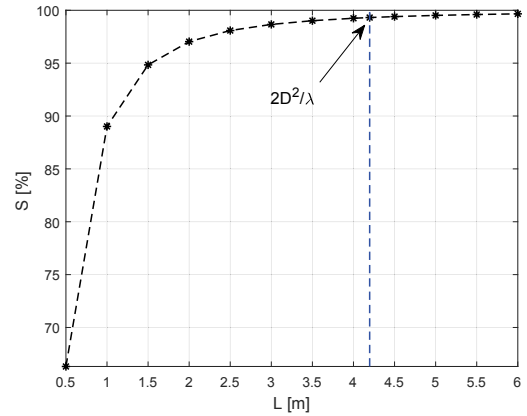


Fig. 3. The pattern similarity for a specular path from DUT boresight direction with various measurement ranges L .

B. Determine number of OTA probes Q

The beam pattern similarity S defined in (9) is utilized as the FoM to determine the number of OTA probes Q and number of active OTA probes K .

For the sake of generality and simplicity, the OTA probes are uniformly distributed on the sectorized spherical surface of interest, where the origin of the sphere is the center of the DUT, and the radius is $L = 1$ m. In the following discussion, a non-line of sight (NLOS) channel model CDL-B and a line of sight (LOS) channel model CDL-E are taken as examples. It is noted that either CDL-B or CDL-E channel model is a single user scenario. The definition of CDL-B and CDL-E are provided in [10], where only the clusters falling into the angular sector of interest are considered here. CDL-B channel model is composed of 21 clusters with the dynamic power range of 11.4 dB. CDL-E channel model consists of 14 clusters with a dynamic power range of 29.8 dB. Note that we use the Laplacian power weighting to generate the cluster PAS [11].

The beamforming power pattern under channel model CDL-B and CDL-E with two sampling densities are shown in Fig. 4(a) and 5(a), respectively. The two sampling densities, i.e., 5° and 10° in both azimuth and elevation domain are utilized,

where the number of OTA probes Q is $(\frac{180}{5} + 1) \times (\frac{60}{5} + 1) = 481$ and $(\frac{180}{10} + 1) \times (\frac{60}{10} + 1) = 133$, respectively. As can be seen, for both cases, the higher the sampling density, the larger the beam pattern similarity can be achieved, i.e., the emulated beam pattern gets closer to the target beam pattern. However, on the other side, a high sampling density also implies a large set of OTA probes, which will increase the system cost and complexity. Note that for LOS case as CDL-E model, the accuracy of the emulated channel is highly determined by whether there exists an active OTA probe at the dominant direction and the measurement range L .

The respective PAS for CDL-B and CDL-E channel models are shown in Fig. 4(b) and 5(b), respectively. In both Fig. 4(b) and 5(b), the top figure is the continuous target PAS. The figures with the title of "5°, $Q = 481$, PAS" and "10°, $Q = 133$, PAS" display the optimal power distribution over the 481 and 133 OTA probes to reconstruct the target PAS, respectively. Note that, in Fig. 4(b) and 5(b), the power range is set to be 60 dB for both 5° and 10° sampling densities, and therefore some probes with very small power are not shown in the figures.

C. Determine number of active OTA probes K

In this section, the number of active OTA probes K is set to 8. Therefore, the objective is to select 8 active probes from 481 or 133 available OTA probes defined before. In this paper, the particle swarm optimization (PSO) algorithm is utilized to find the optimal subset of 8 active OTA probes from the Q OTA probes [12]. The beamforming power pattern under channel model CDL-B and CDL-E with 8 active OTA probes are shown in Fig. 4(a) and 5(a), respectively. Comparing these two figures, we can see that for a high directive channel model as CDL-E, only limited number of probes are dominant and therefore a small K can be sufficient. However, with a more uniform channel model as CDL-B, a larger K should be expected. Furthermore, the respective PAS produced by 8 active OTA probes to mimic CDL-B and CDL-E channel models are plotted in Fig. 4(b) and 5(b), respectively. The 8 active probes are selected from the Q OTA probes and assigned the optimal power weights by PSO algorithm to reproduce the target PAS as best as the MPAC setup can. Both figures show the effectiveness of the PSO algorithm for active OTA probe selection. With the PSO algorithm, the probes, which are dominant in synthesizing the radio channel, are selected. For the LOS case as CDL-E channel model shown in Fig. 5(b), even though the number of active probes is set to be 8, some of the probes are with very weak power, meaning that the required number of active probes is less than 8.

V. CONCLUSIONS

The MPAC setup has great potential for OTA testing of massive MIMO BS. However, a major concern for the MPAC system is that the system cost might be overwhelming. In this paper, we propose a 3D sectorized MPAC setup with a limited number of active OTA probes for massive MIMO BS performance testing. A complete solution for designing the

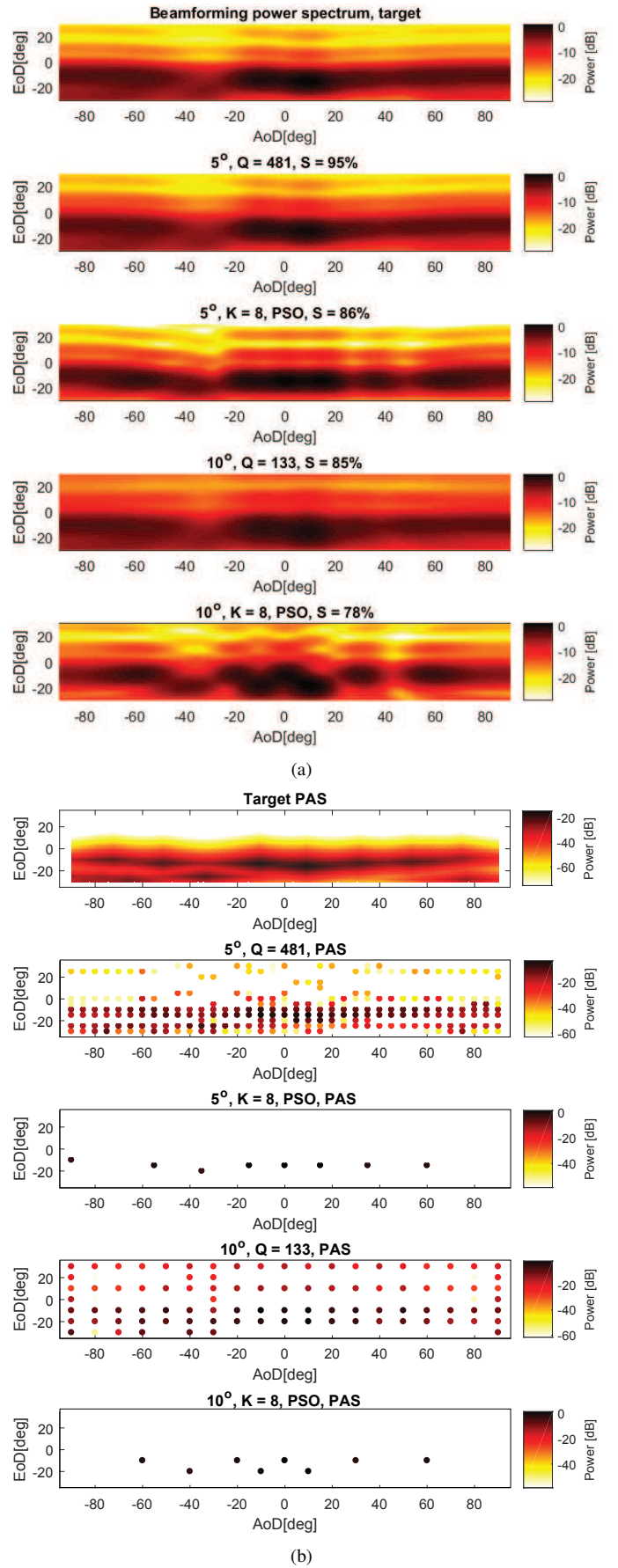


Fig. 4. For channel model CDL-B with the measurement range $L = 1$ m, (a) beamforming power pattern (b) PAS.

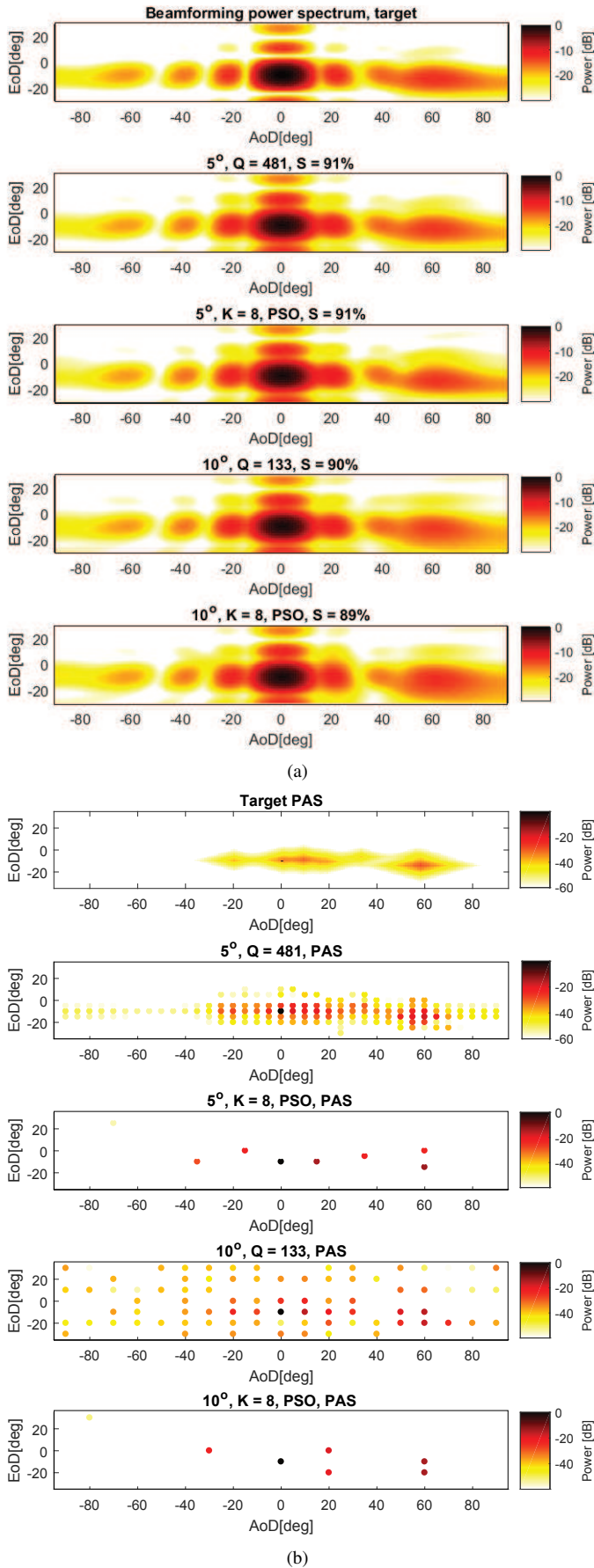


Fig. 5. For channel model CDL-E with the measurement range $L = 1$ m, (a) beamforming power pattern (b) PAS.

low-cost MPAC system is proposed based on TR 38.901 CDL models. A set of the CDL models is mostly a concern to be able to compare performance for different setups, since the channel parameters remain static. A DUT with an 8×8 planar array of half-wavelength element spacing placed on the vertical plane is taken as an example to illustrate the determination of the key design parameters. The designed parameters are found as follows: measurement range $L = 1$ m; OTA probe configurations for 5° and 10° sampling densities are with 481 and 133 OTA probes, respectively; the number of active OTA probes is set to be 8.

ACKNOWLEDGMENT

This work has been partially supported by Huawei Technologies Sweden AB, Gothenburg, Sweden. Dr. Wei Fan would like to acknowledge the financial assistance from Danish council for independent research (grant number: DFF 611100525).

REFERENCES

- [1] E. G. Larsson, O. Edfors, F. Tufvesson, and T. L. Marzetta, "Massive mimo for next generation wireless systems," *IEEE Communications Magazine*, vol. 52, no. 2, pp. 186–195, 2014.
- [2] W. Fan, P. Kyösti, L. Hentilä, and G. F. Pedersen, "MIMO Terminal Performance Evaluation With a Novel Wireless Cable Method," *IEEE Transactions on Antennas and Propagation*, vol. 65, no. 9, pp. 4803–4814, 2017.
- [3] W. Yu, Y. Qi, K. Liu, Y. Xu, and J. Fan, "Radiated two-stage method for LTE MIMO user equipment performance evaluation," *IEEE Transactions on Electromagnetic Compatibility*, vol. 56, no. 6, pp. 1691–1696, 2014.
- [4] X. Chen, "Throughput modeling and measurement in an isotropic-scattering reverberation chamber," *IEEE Transactions on Antennas and Propagation*, vol. 62, no. 4, pp. 2130–2139, 2014.
- [5] W. Fan, F. Zhang, T. Jämsä, M. Gustafsson, P. Kyösti, and G. F. Pedersen, "Reproducing standard some channel models for massive mimo base station radiated testing," in *Antennas and Propagation (EUCAP), 2017 11th European Conference on*. IEEE, 2017, pp. 3658–3662.
- [6] P. Kyösti, T. Jämsä, and J.-P. Nuutinen, "Channel modelling for multi-probe over-the-air mimo testing," *International Journal of Antennas and Propagation*, 2012.
- [7] P. Kyösti, W. Fan, G. F. Pedersen, and M. Latva-Aho, "On dimensions of ota setups for massive mimo base stations radiated testing," *Ieee Access*, vol. 4, pp. 5971–5981, 2016.
- [8] P. Kyösti, T. Jämsä, and J.-P. Nuutinen, "Channel modelling for multi-probe over-the-air mimo testing," *International Journal of Antennas and Propagation*, vol. 2012, 2012.
- [9] P. Kyösti, Hentilä, W. Fan, J. Lehtomäki, and M. Latva-Aho, "On radiated performance evaluation of massive mimo devices in multi-probe anechoic chamber ota setups," *submitted to IEEE transactions on antennas and propagation*.
- [10] TR38.901, "5g; study on channel model for frequencies from 0.5 to 100 ghz," *3GPP, Tech. Rep. Rel 14, V14.0.0*, June, 2017.
- [11] W. Fan, T. Jämsä, J. Ø. Nielsen, and G. F. Pedersen, "On angular sampling methods for 3-d spatial channel models," *IEEE Antennas and Wireless Propagation Letters*, vol. 14, pp. 531–534, 2015.
- [12] J. Robinson and Y. Rahmat-Samii, "Particle swarm optimization in electromagnetics," *IEEE transactions on antennas and propagation*, vol. 52, no. 2, pp. 397–407, 2004.